ACS Photonics

Article

pubs.acs.org/journal/apchd5

Electric Field-Induced High Order Nonlinearity in Plasmonic Nanoparticles Retrieved with Time-Dependent Density Functional Theory

Garikoitz Aguirregabiria,[†] Dana Codruta Marinica,[‡] Ruben Esteban,[§,∥] Andrey K. Kazansky,[§,∥] Javier Aizpurua,[§] and Andrei G. Borisov*[,‡]

[†]Material Physics Center CSIC-UPV/EHU, Paseo Manuel de Lardizabal 5 20018, Donostia-San Sebastián, Spain

[‡]Institut des Sciences Moléculaires d'Orsay, UMR 8214 CNRS-Université Paris-Sud, Bâtiment 351, 91405 Orsay Cedex, France

[§]Material Physics Center CSIC-UPV/EHU, Donostia International Physics Center DIPC, Paseo Manuel de Lardizabal 5 20018, Donostia-San Sebastián, Spain

[∥]IKERBASQUE, Basque Foundation for Science, 48013 Bilbao, Spain

Supporting Information

ABSTRACT: The nonlinear response of metallic nanoparticles is obtained from quantum time dependent density functional theory calculations. Without any aprioristic assumption our calculations allow us to identify high-order harmonic generation in canonical plasmonic structures such as spherical single particles and dimers. Furthermore, we demonstrate that under currently available experimental conditions, the application of an external polarizing field to the nanoparticles allows to actively control even-order harmonic generation in otherwise symmetry forbidden situations. Our quantum calculations provide quantitative access to the high-order response of metallic nanoantennas, which is of utmost importance in the design, control, and exploitation of optoelectronic devices as well as in the generation of extreme ultraviolet radiation.

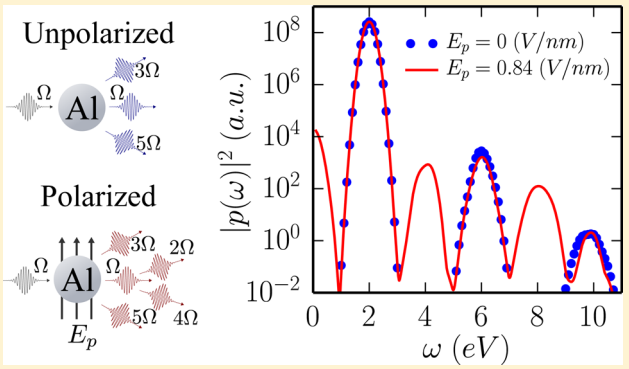

KEYWORDS: *plasmonics, nonlinear optics, nanoantennas*

Coupling of light and collective electronic excitations in metal nanoparticles (localized plasmons) allows to manipulate optical fields well below the diffraction limit, stimulating an active research activity in nanophotonics.[1,2] Many theoretical and experimental studies have shown the advantage of using plasmonic nanostructures in field-enhanced spectroscopy and sensing,[3,4] design of single photon sources,[5,6] light harvesting and photochemistry,[7−10] and nonlinear optics.[11−22] These and many other practical applications have been driven by the technological progress that allows nowadays to engineer nanostructures with desired optical properties.[23,24] Along with a "passive" tailoring during the fabrication process, the ability to actively modify the linear and nonlinear response of plasmonic nanostructures opens new capabilities of paramount importance in nanophotonics. In particular, the electrical control of the optical response of metallic building nanoblocks, similar to that available in two-dimensional (2D) materials,[25] would allow their integration into optoelectronic devices providing compact signal processing and information transfer.

A variety of strategies of active control of the optical response have been proposed in the linear regime,[26−29] and the possibility of electrical tuning of plasmon resonances by means of different physical mechanisms has been recently demonstrated.[30−39] In this context, with the exception of optical rectification,[40−42] the nonlinear regime remains largely unexplored. It is only recently that experimental evidence of electrically controlled second harmonic generation has been reported in planar metamaterials and plasmonic nanocavities filled with nonlinear material.[43,44]

Here we use the time-dependent density functional theory (TDDFT) to retrieve the generation of high-order harmonics in small spherical plasmonic nanoparticles and nanoparticle dimers. The quantum description of valence electrons in TDDFT calculations allows us to go beyond traditional or newly developed time-domain approaches based on classical electrodynamic theories or on the hydrodynamic model.[11,12,22,45−50] Our work should thus provide a benchmark for further theoretical developments. We study the high-order harmonic generation and its dependence on applied electric field and plasmon resonances. We also demonstrate the advantage of using a nanoantenna geometry characterized by

Received: December 1, 2016
Published: February 2, 2017

DOI: 10.1021/acsphotonics.6b00953
ACS Photonics 2017, 4, 613−620

narrow plasmonic gaps. While some of these issues have been discussed in numerous experimental and theoretical papers,[13,14,16,19,20,22,45,51−55] to our knowledge, this is the first time that full quantum calculations allow their quantitative assessment. We find a robust field-induced second harmonic generation,[43,44,55−58] in centrosymmetric nanostructures, and demonstrate the possibility of a controllable and efficient generation of higher harmonics under achievable experimental conditions. To this end, we consider aluminum nanoparticles, which offer several advantages because of their strong nonlinearity[59,60] and the presence of a Mie plasmon resonance in the ultraviolet,[61−63] so that the nonlinear signal can be resonantly enhanced using a pump laser in the visible or near-infrared range of the spectrum. We also show that because of the field enhancement in a narrow junction between nanoparticles, the dimer configuration allows to increase the efficiency of electric field-induced even-order harmonic generation (EFIEHG) by orders of magnitude compared to that obtained in individual nanoparticles. The results of our study establish a theoretical framework to develop electrically controllable ultracompact nonlinear optical devices.

RESULTS AND DISCUSSION

Electrical Control of the Nonlinear Response. Let us first recall the main principles of electrical control of high harmonic generation. The optical response of a nanostructure much smaller than the wavelength of light can be described by means of the induced dipole **p**. Consider a nanostructure made of centrosymmetric material, with a geometry characterized by a reflection symmetry plane set as the (x,y)-plane. For a z-polarized incident electromagnetic field, the induced dipole at frequency ω is given by[64]

$$\mathbf{p}_\omega = \sum_i \hat{e}_i \left[\alpha^{(1)}_{iz}(\omega)E_\omega + \alpha^{(3)}_{izzz}(\omega;\, \omega_o,\, \omega_k,\, \omega_m)E_{\omega_o}E_{\omega_k}E_{\omega_m} + \ldots\right] \tag{1}$$

where the subindex i indicates the spatial direction $i = \{x, y, z\}$, and $\hat{e}_i$ is the unit length vector in the corresponding direction. The $\alpha^{(n+1)}$ (n = 0, 2, 4, 6, ...) are the linear and nonlinear polarizability tensors of the system, where only the odd orders are nonzero because of the symmetry, and $\omega = \omega_o + \omega_k + \omega_m$. The different ω frequency components of the fields are denoted as E_ω. The combination of the different terms shows that only odd-order harmonics can be generated in a centrosymmetric system.

Even-order harmonics can be obtained if, along with the incident electromagnetic wave, the nanostructure is subjected to a polarizing static electric field $\mathbf{E}_p = \hat{e}_z E_p$ that breaks the symmetry. For a spherical nanoparticle illuminated by monochromatic light the corresponding nonlinear dipoles can be obtained from eq 1 in a scalar form as

$$\begin{aligned} p_{2\Omega} &= \alpha^{(3)}(2\Omega)E^2_\Omega E_p, \\ p_{4\Omega} &= \alpha^{(5)}(4\Omega)E^4_\Omega E_p \end{aligned} \tag{2}$$

where we used the following simplified notations:

$$\begin{aligned} \alpha^{(3)}(2\Omega) &\equiv \alpha^{(3)}(2\Omega;\, \Omega,\, \Omega,\, 0), \\ \alpha^{(5)}(4\Omega) &\equiv \alpha^{(5)}(4\Omega;\, \Omega,\, \Omega,\, \Omega,\, \Omega,\, 0) \end{aligned} \tag{3}$$

Only lower order contributions to the nonlinear dipole are considered here. Since the power radiated by the dipole is given by $I_{n\Omega} = \frac{(n\Omega)^4}{3c^3}|p_{n\Omega}|^2$ (c is the speed of light), it follows from eq 2 that the intensities of the even-order harmonics can be actively controlled by means of the polarizing field E_p:

$$I_{n\Omega} = \frac{(n\Omega)^4}{3c^3}|\alpha^{(n+1)}(n\Omega)E^n_\Omega|^2 E^2_p, \quad n = 2,\, 4,\, 6,\, \ldots \tag{4}$$

where $\frac{c}{4\pi}|E_\Omega|^2$ is the intensity of the excitation source.

In a practical situation, the metal nanoparticles are typically deposited at the substrate and do not have the ideal geometry so that the inversion symmetry is generally broken. Along with the generation of the even-order harmonic signal controlled by an applied electric field, the symmetry breaking would lead to the "background" even-order harmonic signal, as has been observed experimentally.[43,44] In this work we address only the former (EFIEHG) process assuming that both contributions can be distinguished by varying the strength of the applied electric field.[43,44]

Single Nanoparticle. Our calculations are performed within the TDDFT framework well suited to describe the nonlinear response of nanostructures at a quantum level.[65] This allows us to quantitatively determine the relevant physical quantities and their dependence on the plasmon modes of the system, as well as on the applied electric field. The Kohn−Sham (KS) scheme of TDDFT is used, along with the adiabatic local density approximation for the exchange-correlation potential.[66] Retardation effects are neglected because of the small particle sizes addressed in this work. In this section we study the valence electron dynamics in individual Aluminum spherical nanoparticles and discuss sphere dimers in the next section. The particles are placed in vacuum. The effect of the surrounding aluminum oxide shell typically formed in ambient conditions[63] is not considered here. Aluminum is a prototype of a free-electron metal well described by the jellium model (JM)[67,68] that we adopt for our study. Despite its simplicity, the JM correctly captures the collective behavior of the conduction electrons and allows to address linear and nonlinear effects in plasmonic structures.[69−71] Within the JM, the lattice ions are represented with a uniform positive background charge of the density $n_+ = \left[\frac{4\pi}{3}r_s^3\right]^{-1}$, where r_s = 1.1 Å is the Wigner-Seitz radius. Thus, the neutral spherical nanoparticle comprising N_e = 2018 electrons has a radius R_{cl} = 13.86 Å, where the sphere of radius R_{cl} provides the position of the jellium edge separating positive background charge from the vacuum. Further details on the present numerical implementation can be found in ref 69, and it is also provided in the Supporting Information.

The electron density dynamics in the system is triggered by an incident electromagnetic pulse polarized along the direction of the applied static field E_p. The total electric field acting on the nanostructure is given by

$$E(t) = E_p + E_0 \cos(\Omega t)e^{-(t-t_0)^2/\tau^2} \tag{5}$$

where the second term describes a Gaussian electromagnetic pulse with duration 2τ. The latter is set large enough (typically 6 laser periods or 10−20 fs) so that well-resolved harmonics can be observed in the spectrum of the induced dipole.[49] We use optical pulses of intensity $\mathcal{P} = 10^{11}$ W/cm^2 and $\mathcal{P} = 10^{12}$ W/cm^2 so that $E_0 = 1.51 \times 10^{-3}$ a.u. and $E_0 = 4.8 \times 10^{-3}$ a.u., correspondingly. Here, "a.u." stands for atomic units (1 a.u. = 514 V/nm).

DOI: 10.1021/acsphotonics.6b00953
ACS Photonics 2017, 4, 613−620

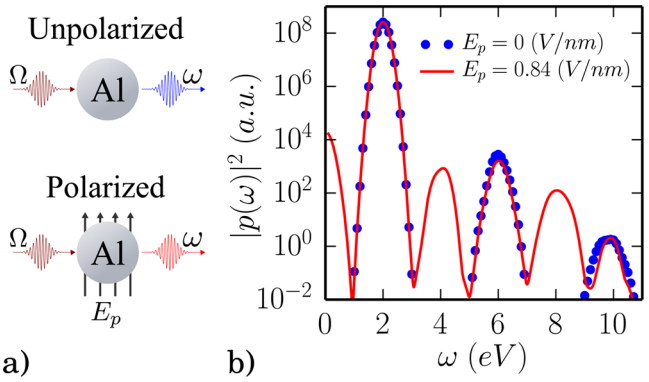

Figure 1. (a) Sketch of the spherical aluminum nanoparticle subjected to an optical pulse of frequency Ω. Unpolarized/polarized case refers to the situation without/with the presence of an applied static field E_p. (b) Intensity spectrum of the induced dipole $|p_\omega|^2$ (in atomic units, a.u.) for a spherical aluminum nanoparticle of radius R_{cl} = 13.86 Å excited by an optical pulse of intensity $\mathcal{P} = 10^{12}$ W/cm^2, frequency Ω = 2 eV (620 nm), and polarized along E_p. Blue and red colors indicate results obtained for the "Unpolarized", E_p = 0, and "Polarized", E_p = 0.843 V/nm (0.0016 a.u.), case.

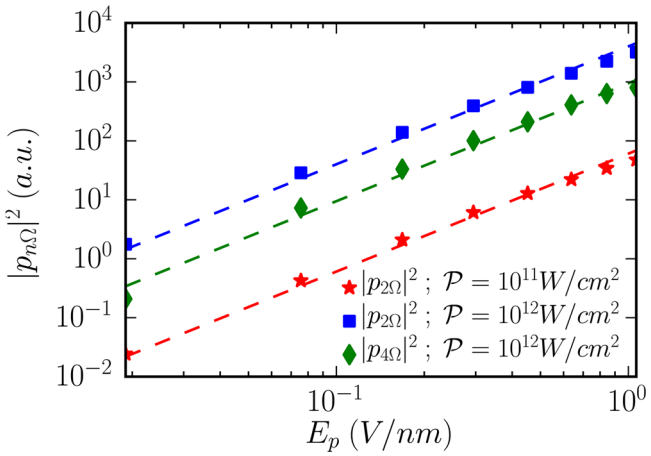

Figure 2. TDDFT results of the nonlinear response of a R_{cl} = 13.86 Å spherical Al nanoparticle. The intensities of nonlinear dipoles at the 2nd ($|p_{2\Omega}|^2$) and 4th ($|p_{4\Omega}|^2$) harmonic frequencies are presented as functions of the strength of the applied static field E_p. Symbols: TDDFT results, dashed lines: fits by the quadratic dependence. The incident optical pulse with frequency Ω = 2.18 eV (568.7 nm) is polarized along the direction of E_p. Results are shown for two powers of the incident pulse: $\mathcal{P} = 10^{12}$ W/cm^2, and $\mathcal{P} = 10^{11}$ W/cm^2. For further details see the inset.

The effect of the polarizing field E_p on the nonlinear response of the spherical Al nanoparticle is shown in Figure 1. The intensity spectrum $|p(\omega)|^2$ of the dipole induced by the electromagnetic pulse is presented for the cases with and without polarizing field. The results are shown in atomic units (a.u.). $p(\omega)$ is obtained by the time-to-frequency Fourier transform of the induced dipole $p(t)$ calculated with TDDFT upon subtraction of the static polarization produced by E_p. Without the polarizing field only the odd-order harmonics are excited as expected from the symmetry of the system (blue dots). We clearly distinguish up to the fifth harmonic in the spectrum where the finite size of the harmonics peaks reflects the Gaussian profile of the incident optical pulse[49] (see eq 5). When the static field is applied to the nanoparticle, even-order harmonics at $\omega = 2\Omega$ and 4Ω emerge (red lines). Observe that also the static polarization is produced via $\alpha^{(3)}(0;\Omega,-\Omega,0)$ type processes. Calculations performed with different powers of the electromagnetic pulse confirm that the intensities of harmonics at $n\Omega$ vary as $\mathcal{P}^n$.

The analysis of the electrical control of the even-order harmonic generation using a spherical Al nanoparticle is presented in Figure 2. We show the nonlinear dipole induced at the second ($|p_{2\Omega}|^2 \equiv |p(\omega = 2\Omega)|^2$), and the fourth ($|p_{4\Omega}|^2 \equiv |p(\omega = 4\Omega)|^2$) harmonic of the incident optical pulse with frequency Ω = 2.18 eV (wavelength 568.7 nm). The optical frequency is set such that the fourth harmonic is at resonance with the dipolar plasmon mode of the Al nanosphere, $4\Omega = \Omega_D$. The energy of the dipolar plasmon Ω_D = 8.72 eV (142.2 nm) is defined as the position of the maximum of the optical absorption cross section calculated here with TDDFT (see Figure 3). The resonance condition results in the strong increase of the nonlinear signal as we discuss below. In agreement with eqs 2 and 4, the calculated nonlinearity (symbols) shows the $|p_{n\Omega}|^2 \propto E_p^2$ dependence with applied static field E_p as follows from the comparison with the analytical fit given by the dashed lines. Thus, the 10^4 increase in the intensities of the emitted harmonics has been obtained within the studied range of E_p. The 2 orders of magnitude difference in the second harmonic intensity obtained with incidence pulses of the intensity $\mathcal{P} = 10^{12}$ W/cm^2 and $\mathcal{P} = 10^{11}$ W/cm^2 reflects the $\propto\mathcal{P}^2$ scaling of the nonlinear signal (see eq 4).

The TDDFT results in Figure 2 span the 0.02 V/nm ≤ E_p ≤ 1 V/nm (4×10^{-5} a.u. ≤ E_p ≤ 2×10^{-3} a.u.) range, so that the relative strength of the optical and applied static fields is 0.01 ≤ E_p/E_0 ≤ 1. While one can a priori use eq 2 and extrapolate the data to even smaller E_p, in the TDDFT calculations for our nanoparticle, the even-order harmonics are resolved for applied static fields above 0.02 V/nm. These values of the polarizing field require that the nanostructure is placed in metallic nanogaps such as break junction or gap of electrically connected dimer antenna.[40,42,72,73] In this case, an applied bias of a few volts can create strong enough static fields across the nanogap. An additional benefit of using an electrically connected dimer antenna is that the incident optical field acting on the Al nanostructure can be resonantly enhanced thus increasing the frequency conversion efficiency.

The analytical fit of the TDDFT results with eq 2 allows to extract the hyperpolarisabilities of the nanosphere $|\alpha^{(3)}(2\Omega)|$ = 2.62×10^7 a.u. (1.3×10^{-32} esu), and $|\alpha^{(5)}(4\Omega)| = 2.5 \times 10^{12}$ a.u. (4.1×10^{-42} esu), as well as the respective effective susceptibilities (polarizability per unit volume) $|\chi^{(3)}(2\Omega)| = 1.2 \times 10^{-12}$ esu and $|\chi^{(5)}(4\Omega)| = 10^{-22}$ esu. We also obtained that $|\alpha^{(3)}(3\Omega;\Omega,\Omega,\Omega)|$ driving the third harmonic generation process is of the same order of magnitude as $|\alpha^{(3)}(2\Omega)|$. The values above are given for Ω = 2.18 eV (568.7 nm) such that the 4Ω frequency coincides with the plasmon resonance. The third-order nonlinearity calculated here for an Al nanosphere is typically 4 orders of magnitude lower than the theoretical results reported for graphene nanostructures,[74] and it is comparable to the typical values for gold[75−77] and silver.[78] Note, however, that in this latter case, $|\chi^{(3)}(3\Omega)| = 2 \times 10^{-9}$ esu was reported for the fundamental frequency Ω = 2.95 eV (420 nm) at resonance with Ag nanoparticle plasmon.[79]

The possibility of strong enhancement of nonlinear signal when the sought harmonic matches the plasmon resonance of the nanostructure represents a major advantage when using

DOI: 10.1021/acsphotonics.6b00953
ACS Photonics 2017, 4, 613−620

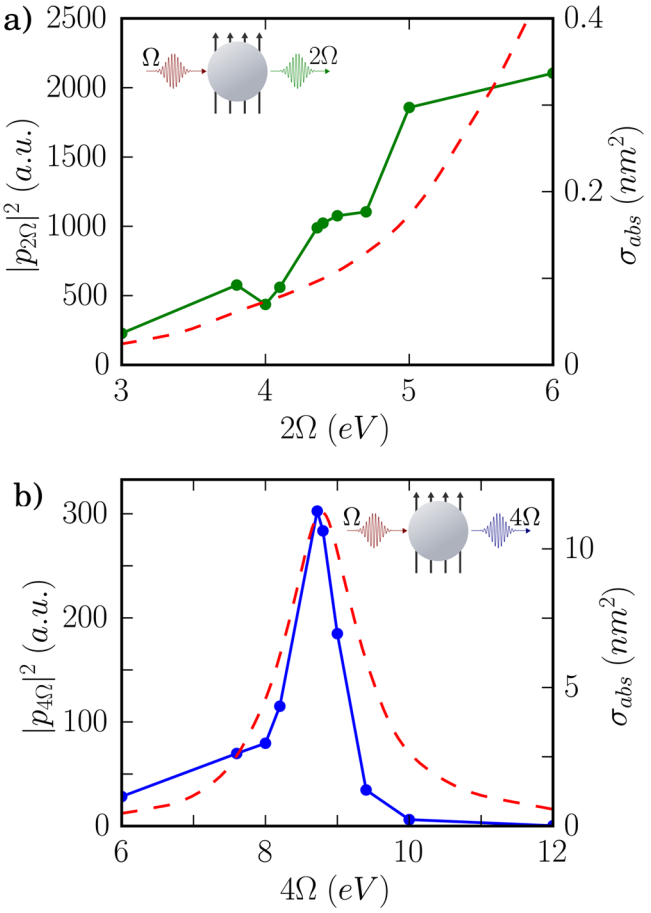

Figure 3. TDDFT results for the linear and nonlinear responses of a R_{cl} = 13.86 Å Al spherical nanoparticle. The data are shown as a function of the 2nd harmonic frequency 2Ω (panel a), and 4th harmonic frequency 4Ω (panel b). Green line with circles in panel (a): intensity of the nonlinear dipole $|p_{2\Omega}|^2$; Blue line with circles in panel (b): intensity of the nonlinear dipole $|p_{4\Omega}|^2$. An incident optical pulse at frequency Ω has an intensity $\mathcal{P} = 10^{12}$ W/cm^2 and the static field E_p = 0.843 V/nm (0.0016 a.u.) is applied. Dashed red line: optical absorption cross-section of the individual Al nanoparticle $\sigma_{abs}(\omega = 2\Omega)$ (panel a), and $\sigma_{abs}(\omega = 4\Omega)$ (panel b).

plasmonic nanoparticles. This effect is usually discussed for the 2nd or 3rd harmonic generation.[16,20,49,51−53,74,76−79] In this respect, Al nanoparticles offer appealing possibilities because of the high density of the conduction electrons which lead for small nanoparticles to plasmon frequencies in the ultraviolet allowing to reach resonance conditions for the 4th or higher harmonics. We can link the linear and nonlinear response of Al nanoparticles with help of the results shown in Figure 3. In this figure we plot the optical absorption cross section σ_{abs} calculated here with TDDFT as well as the intensity of the nonlinear dipole at 2nd $|p_{2\Omega}|^2$ (panel a) and 4th $|p_{4\Omega}|^2$ (panel b) harmonic produced by an incident electromagnetic pulse when a static field with E_p = 0.843 V/nm is applied. The results are shown as a function of the 2nd and 4th harmonic frequency, 2Ω and 4Ω, correspondingly. Since static and optical fields are constant, the data in Figure 3 shows equivalently the frequency evolution of the hyperpolarizabilities as follows from eq 4.

The absorption cross-section features the dipolar plasmon resonance at Ω_D = 8.72 eV (142.2 nm). Excitation of this mode affects the nonlinear response of the nanosphere. Indeed, within the studied frequency range 1.5 eV ≤ Ω ≤ 3 eV, the 2nd harmonic frequency approaches Ω_D from lower energies. Consistently, the intensity of the 2nd harmonic increases with increasing Ω, following the frequency dependence of the absorption cross-section. The nonmonotonous behavior of the intensity of the nonlinear dipole stems from the quantization of the electronic states in the spherical cluster. As to the 4th harmonic, its frequency range overlaps Ω_D. In this case, the intensity of the nonlinear dipole $|p_{4\Omega}|^2$ shows a resonance profile with a 10-fold increase when the frequency of the nonlinear polarization matches the dipolar plasmon mode of the nanosphere ($|p_{4\Omega}|^2$ = 303 a.u. at maximum and $|p_{4\Omega}|^2$ = 28 a.u. for Ω = 1.5 eV). For the present system, the resonant enhancement of the 4th harmonic is such that its intensity becomes comparable to the 2nd harmonic intensity for Ω = 2.18 eV.

Nanosphere Dimer. Going beyond the single particle, many applications in photonics, including nonlinear processes, benefit from the strong field enhancement produced in the gaps between metallic nanoparticles.[11−16,43,53] In this respect, the spherical dimer configuration has become a reference system in the analysis of classical and quantum aspects of the optical response in plasmonic nanogaps.[69−71,80] In quest for an increased efficiency of actively controlled EFIEHG, we consider the dimer formed by two identical Al nanospheres of R_{cl} = 11 Å radius each comprising 1000 electrons (see sketch in Figure 4). The dimer contains then nearly the same total amount of electrons as the individual Al nanoparticle discussed in the previous section. We need to consider a smaller size of the nanospheres forming the dimer because of computational constraints as we further discuss in Supporting Information. Because of the symmetry, only odd-order harmonic generation is produced for optical fields polarized along the dimer axis (*z*-axis).[54] Application of the static field $\hat{e}_z E_p$ allows controllable generation of even-order harmonics, where eqs 2 and 4 can be applied for analysis of the results upon assignment of nonlinear polarizabilities to the entire dimer.

In order to characterize the linear optical properties of an Al nanosphere dimer in vacuum, we show in Figure 4a the absorption spectra calculated with TDDFT for varying width of the gap d_{gap}. Overall, the evolution of the plasmon resonances upon closing of the gap reflects the change from capacitive to conductive coupling between the nanoparticles, and it is similar to that obtained in earlier quantum calculations for the dimer system.[69−71,81] The red shift of the bonding dipole (BDP) and quadrupole (BQP) plasmon modes is followed by their progressive attenuation and, for the nearly touching geometry, the charge transfer plasmon modes (CTP and CTP′) emerge. This change of the absorption spectra has been assigned to the electron transfer across narrow gaps so that the nanoparticles appear connected prior to the direct geometrical contact between their surfaces.[69,70] As a second effect of the electron transfer across the gap, the plasmon-induced charges at facing surfaces of the nanoparticles are partially neutralized, so that the field enhancement in the gap is reduced.

The nonlinear response of the nanosphere dimer polarized by the static field applied along the dimer axis is analyzed in Figure 4b. The intensity of the second harmonic $|p_{2\Omega}|^2$ is shown in this figure as a function of the width of the gap for two different frequencies of the incident pulse, Ω = 1 eV and 2 eV. The frequency range is chosen such that the analysis is not complicated by the resonant excitations in the system. The results obtained for the dimer are compared to the expected second harmonic intensity of two noninteracting (NI) Al

DOI: 10.1021/acsphotonics.6b00953
ACS Photonics 2017, 4, 613−620

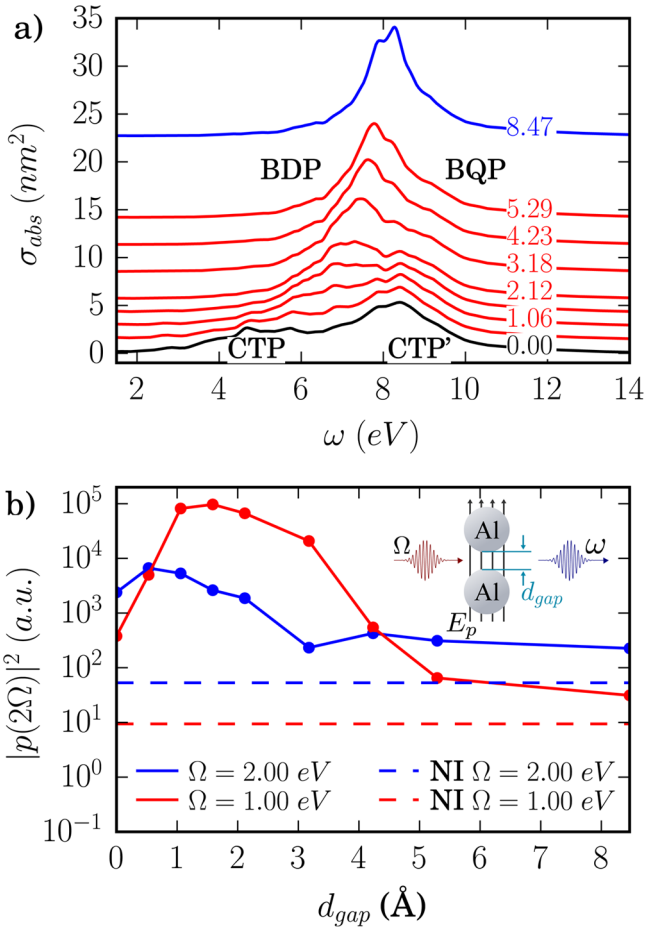

Figure 4. (a) Waterfall plot of the frequency-dependent optical absorption cross section σ_{abs} calculated with TDDFT for an Al nanosphere dimer in vacuum. The incoming electromagnetic plane wave is polarized along the dimer axis (z-axis). Absorption spectra are labeled according to the corresponding size of the gap between nanoparticles d_{gap} (given in Å). For clarity, a vertical shift proportional to d_{gap} is introduced for each absorption spectrum. (b) Intensity of the nonlinear dipole at the 2nd harmonic, $|p_{2\Omega}|^2$, as a function of the width of the gap for two different frequencies of the z-polarized $\mathcal{P} = 10^{11}$ W/cm^2 incident pulse. Red line with dots, Ω = 1 eV (1240 nm), and blue line with dots, Ω = 2 eV (620 nm). A static field E_p = 0.843 V/nm (0.0016 a.u.) is applied along the z-axis. Dashed lines of the corresponding colors show the expected value for two noninteracting nanospheres (NI) under the same illumination conditions.

nanospheres of R_{cl} = 11 Å radius (4× single sphere result). It follows from our calculations that the generation of even-order harmonics in the dimer configuration is much more efficient than in individual nanoparticles.

Already at large separations, d_{gap}, the coupling between the nanospheres in the dimer increases the nonlinear signal as compared to the noninteracting system. As d_{gap} is reduced, the nonlinearity is increased by orders of magnitude. We attribute this effect to the strong field enhancement in the gap region as well as to the nonlinearity of the tunneling current between nanoparticles.[69,82] The $|p_{2\Omega}|^2$ reaches a maximum for $d_{gap} \simeq 1.5$ Å. For the narrowest gaps, the junction acquires conductive character,[69,70,81] and the system evolves into the limit of a continuous metal nanostructure. In this situation the effects of the gap are reduced, with the field enhancement quenched,[69,70,81] thus, leading to less efficient second harmonic generation. We leave for future report the detailed analysis of the frequency and geometry evolution of the nonlinear response, as well as its sensitivity to the electron tunneling and plasmon modes of the dimer. It is worthwhile mentioning here that we retrieve similar qualitative behavior of the nonlinearity with gap size as was measured previously by four-wave mixing and 3rd harmonic generation.[14,19]

CONCLUSIONS AND OUTLOOK

In conclusion, we used quantitative first-principles calculations to study the nonlinear response of plasmonic nanoparticles. Our quantum approach goes beyond the classical and hydrodynamic descriptions of high harmonic generation. It therefore allows quantitative assessment of the role of an external applied field, the spectral matching with plasmon resonances, and the presence of narrow plasmonic gaps. In particular, we have revealed the possibility of developing active electrical control of nonlinear processes in plasmonic nanoparticles in currently available experimental conditions.

We have shown that Al nanoparticles and nanoparticle dimers are promising systems for the realization of controllable even-order high-harmonic generation via an applied dc electric field. The necessary conditions for frequency conversion can be reached, for instance, by placing an Al nanosystem in a break junction or in a gap of electrically driven plasmonic gold nanoantenna.[73] The latter should be particularly efficient as it allows in principle to reach a double resonance condition, where the fundamental frequency is resonant with the gold nanoantenna and the high-order harmonic is at resonance with the plasmon mode of the Al nanostructure. Indeed, for the particle sizes considered here we have demonstrated that for the fundamental frequency in the visible or infrared range, the fourth or higher harmonics can be set into resonance with the plasmon mode of the Al nanostructure, resulting in order of magnitude enhancement of the nonlinear response. We have also demonstrated that because of the field enhancement and electron tunneling in narrow gaps between metallic nanoobjects, the dimer configuration allows to increase the intensity of the second harmonic signal by up to 3 orders of magnitude as compared to that of the individual nanoparticles. Our quantitative study thus not only offers the appropriate quantum theoretical treatment of nonlinear processes in plasmonic systems induced by an applied electric field, but it also establishes an effective platform to design and exploit electrically controllable nonlinear devices for optoelectronics and extreme ultraviolet generation.

ASSOCIATED CONTENT

Supporting Information

The Supporting Information is available free of charge on the ACS Publications website at DOI: 10.1021/acsphotonics.6b00953.

Detailed description of the TDDFT calculations and extraction of the nonlinear response of metallic nanoparticles (PDF).

AUTHOR INFORMATION

Corresponding Author

*E-mail: andrei.borissov@u-psud.fr. Phone: +33 (0)1 69157697.

ORCID

Andrei G. Borisov: 0000-0003-0819-5028

DOI: 10.1021/acsphotonics.6b00953
ACS Photonics 2017, 4, 613−620

Notes

The authors declare no competing financial interest.

■ ACKNOWLEDGMENTS

J.A. acknowledges financial support from the Department of Education of the Basque Government through Project IT756/13 for consolidated groups, Project FIS2016-80174-P from the Spanish Ministry of Economy and Competitiveness, and Federal Grant 70NANB15H321 from the National Institute of Standards and Technology (NIST). R.E. acknowledges support from the Fellows Gipuzkoa program of the Gipuzkoako Foru Aldundia through FEDER funds "Una manera de hacer Europa". A.K.K. acknowledges financial support from Project FIS2016-76617-P of the Spanish Ministry of Economy and Competitiveness.

■ REFERENCES

(1) Schuller, J. A.; Barnard, E. S.; Cai, W.; Jun, Y. C.; White, J. S.; Brongersma, M. L. Plasmonics for extreme light concentration and manipulation. *Nat. Mater.* **2010**, *9*, 193−204.
(2) Stockman, M. I. Nanoplasmonics: past, present, and glimpse into future. *Opt. Express* **2011**, *19*, 22029−22106.
(3) Nie, S.; Emory, S. R. Probing single molecules and single nanoparticles by Surface-Enhanced Raman Scattering. *Science* **1997**, *275*, 1102−1106.
(4) Langer, J.; Novikov, S. M.; Liz-Marzán, L. M. Sensing using plasmonic nanostructures and nanoparticles. *Nanotechnology* **2015**, *26*, 322001.
(5) Esteban, R.; Teperik, T. V.; Greffet, J. J. Optical patch antennas for single photon emission using surface plasmon resonances. *Phys. Rev. Lett.* **2010**, *104*, 026802.
(6) Lian, H.; Gu, Y.; Ren, J.; Zhang, F.; Wang, L.; Gong, Q. Efficient single photon emission and collection based on excitation of gap surface plasmons. *Phys. Rev. Lett.* **2015**, *114*, 193002.
(7) Baffou, G.; Quidant, R. Nanoplasmonics for chemistry. *Chem. Soc. Rev.* **2014**, *43*, 3898−3907.
(8) Ferry, V. E.; Polman, A.; Atwater, H. A. Modeling Light Trapping in Nanostructured Solar Cells. *ACS Nano* **2011**, *5*, 10055−10064.
(9) Clavero, C. Plasmon-induced hot-electron generation at nanoparticle/metal-oxide interfaces for photovoltaic and photocatalytic devices. *Nat. Photonics* **2014**, *8*, 95−103.
(10) Brongersma, M. L.; Halas, N. J.; Nordlander, P. Plasmon-induced hot carrier science and technology. *Nat. Nanotechnol.* **2015**, *10*, 25−34.
(11) Kauranen, M.; Zayats, A. V. Nonlinear plasmonics. *Nat. Photonics* **2012**, *6*, 737−748.
(12) Butet, J.; Brevet, P.-F.; Martin, O. J. F. Optical second harmonic generation in plasmonic nanostructures: from fundamental principles to advanced applications. *ACS Nano* **2015**, *9*, 10545−10562.
(13) Bouhelier, A.; Beversluis, M.; Hartschuh, A.; Novotny, L. Near-field second-harmonic generation induced by local field enhancement. *Phys. Rev. Lett.* **2003**, *90*, 013903.
(14) Danckwerts, M.; Novotny, L. Optical frequency mixing at coupled gold nanoparticles. *Phys. Rev. Lett.* **2007**, *98*, 026104.
(15) Hanke, T.; Krauss, G.; Träutlein, D.; Wild, B.; Bratschitsch, R.; Leitenstorfer, A. Efficient nonlinear light emission of single gold optical antennas driven by few-cycle near-infrared pulses. *Phys. Rev. Lett.* **2009**, *103*, 257404.
(16) Harutyunyan, H.; Volpe, G.; Quidant, R.; Novotny, L. Enhancing the nonlinear optical response using multifrequency gold-nanowire antennas. *Phys. Rev. Lett.* **2012**, *108*, 217403.
(17) Hohenau, A.; Krenn, J. R.; Beermann, J.; Bozhevolnyi, S. I.; Rodrigo, S. G.; Martin-Moreno, L.; Garcia-Vidal, F. Spectroscopy and nonlinear microscopy of Au nanoparticle arrays: Experiment and theory. *Phys. Rev. B: Condens. Matter Mater. Phys.* **2006**, *73*, 155404.
(18) Lippitz, M.; van Dijk, M. A.; Orrit, M. Third-harmonic generation from single gold nanoparticles. *Nano Lett.* **2005**, *5*, 799−802.
(19) Hajisalem, G.; Nezami, M. S.; Gordon, R. Probing the quantum tunneling limit of plasmonic enhancement by third harmonic generation. *Nano Lett.* **2014**, *14*, 6651−6654.
(20) Czaplicki, R.; Mäkitalo, J.; Siikanen, R.; Husu, H.; Lehtolahti, J.; Kuittinen, M.; Kauranen, M. Second-harmonic generation from metal nanoparticles: resonance enhancement versus particle geometry. *Nano Lett.* **2015**, *15*, 530−534.
(21) Mesch, M.; Metzger, B.; Hentschel, M.; Giessen, H. Nonlinear plasmonic sensing. *Nano Lett.* **2016**, *16*, 3155−3159.
(22) Hentschel, M.; Utikal, T.; Giessen, H.; Lippitz, M. Quantitative modeling of the third harmonic emission spectrum of plasmonic nanoantennas. *Nano Lett.* **2012**, *12*, 3778−3782.
(23) Lindquist, N. C.; Nagpal, P.; McPeak, K. M.; Norris, D. J.; Oh, S.-H. Engineering metallic nanostructures for plasmonics and nanophotonics. *Rep. Prog. Phys.* **2012**, *75*, 036501.
(24) Husu, H.; Siikanen, R.; Mäkitalo, J.; Lehtolahti, J.; Laukkanen, J.; Kuittinen, M.; Kauranen, M. Metamaterials with tailored nonlinear optical response. *Nano Lett.* **2012**, *12*, 673−677.
(25) Koppens, F. H. L.; Chang, D. E.; de Abajo, F. J. G. Graphene plasmonics: A platform for strong light-matter interactions. *Nano Lett.* **2011**, *11*, 3370−3377.
(26) Pala, R. A.; Shimizu, K. T.; Melosh, N. A.; Brongersma, M. L. A nonvolatile plasmonic switch employing photochromic molecules. *Nano Lett.* **2008**, *8*, 1506−1510.
(27) Nikolajsen, T.; Leosson, K.; Bozhevolnyi, S. I. Surface plasmon polariton based modulators and switches operating at telecom wavelengths. *Appl. Phys. Lett.* **2004**, *85*, 5833−5835.
(28) Huang, F.; Baumberg, J. J. Actively tuned plasmons on elastomerically driven Au nanoparticle dimers. *Nano Lett.* **2010**, *10*, 1787−1792.
(29) MacDonald, K. F.; Sámson, Z. L.; Stockman, M. I.; Zheludev, N. I. Ultrafast active plasmonics. *Nat. Photonics* **2009**, *3*, 55−58.
(30) Chu, K. C.; Chao, C. Y.; Chen, Y. F.; Wu, Y. C.; Chen, C. C. Electrically controlled surface plasmon resonance frequency of gold nanorods. *Appl. Phys. Lett.* **2006**, *89*, 103107.
(31) Mulvaney, P.; Pérez-Juste, J.; Giersig, M.; Liz-Marzán, L. M.; Pecharromán, C. Drastic surface plasmon mode shifts in gold nanorods due to electron charging. *Plasmonics* **2006**, *1*, 61−66.
(32) Vivekchand, S. R. C.; Engel, C. J.; Lubin, S. M.; Blaber, M. G.; Zhou, W.; Suh, J. Y.; Schatz, G. C.; Odom, T. W. Liquid plasmonics: Manipulating surface plasmon polaritons via phase transitions. *Nano Lett.* **2012**, *12*, 4324−4328.
(33) Brown, A. M.; Sheldon, M. T.; Atwater, H. A. Electrochemical Tuning of the Dielectric Function of Au Nanoparticles. *ACS Photonics* **2015**, *2*, 459−464.
(34) Byers, C. P.; Zhang, H.; Swearer, D. F.; Yorulmaz, M.; Hoener, B. S.; Huang, D.; Hoggard, A.; Chang, W.-S.; Mulvaney, P.; Ringe, E.; Halas, N. J.; Nordlander, P.; Link, S.; Landes, C. F. From tunable core-shell nanoparticles to plasmonic drawbridges: Active control of nanoparticle optical properties. *Science Advances* **2015**, *1*, e1500988.
(35) Marinica, D. C.; Zapata, M.; Nordlander, P.; Kazansky, A. K.; M. Echenique, P.; Aizpurua, J.; Borisov, A. G. Active quantum plasmonics. *Sci. Adv.* **2015**, *1*, e1501095.
(36) Emboras, A.; Niegemann, J.; Ma, P.; Haffner, C.; Pedersen, A.; Luisier, M.; Hafner, C.; Schimmel, T.; Leuthold, J. Atomic scale plasmonic switch. *Nano Lett.* **2016**, *16*, 709−714.
(37) Chen, K.; Razinskas, G.; Feichtner, T.; Grossmann, S.; Christiansen, S.; Hecht, B. Electromechanically tunable suspended optical nanoantenna. *Nano Lett.* **2016**, *16*, 2680−2685.
(38) Dong, S.; Zhang, K.; Yu, Z.; Fan, J. A. Electrochemically programmable plasmonic antennas. *ACS Nano* **2016**, *10*, 6716−6724.
(39) Huang, Y.-W.; Lee, H. W. H.; Sokhoyan, R.; Pala, R. A.; Thyagarajan, K.; Han, S.; Tsai, D. P.; Atwater, H. A. Gate-Tunable Conducting Oxide Metasurfaces. *Nano Lett.* **2016**, *16*, 5319−5325.

DOI: 10.1021/acsphotonics.6b00953
ACS Photonics 2017, 4, 613−620

(40) Ward, D. R.; Hüser, F.; Pauly, F.; Cuevas, J. C.; Natelson, D. Optical rectification and field enhancement in a plasmonic nanogap. *Nat. Nanotechnol.* **2010**, *5*, 732−736.
(41) Arielly, R.; Ofarim, A.; Noy, G.; Selzer, Y. Accurate determination of plasmonic fields in molecular junctions by current rectification at optical frequencies. *Nano Lett.* **2011**, *11*, 2968−2972.
(42) Stolz, A.; Berthelot, J.; Mennemanteuil, M.-M.; des Francs, G. C.; Markey, L.; Meunier, V.; Bouhelier, A. Nonlinear photon-assisted tunneling transport in optical gap antennas. *Nano Lett.* **2014**, *14*, 2330−2338.
(43) Cai, W.; Vasudev, A. P.; Brongersma, M. L. Electrically controlled nonlinear generation of light with plasmonics. *Science* **2011**, *333*, 1720−1723.
(44) Kang, L.; Lan, S.; Rodrigues, S. P.; Brongersma, W.; Mark, L.; Cai, W. Electrifying photonic metamaterials for tunable nonlinear optics. *Nat. Commun.* **2014**, *5*, 4680.
(45) Scalora, M.; Vincenti, M. A.; de Ceglia, D.; Haus, J. W. Nonlocal and quantum-tunneling contributions to harmonic generation in nanostructures: Electron-cloud-screening effects. *Phys. Rev. A: At., Mol., Opt. Phys.* **2014**, *90*, 013831.
(46) Ciracì, C.; Scalora, M.; Smith, D. R. Third-harmonic generation in the presence of classical nonlocal effects in gap-plasmon nanostructures. *Phys. Rev. B: Condens. Matter Mater. Phys.* **2015**, *91*, 205403.
(47) Hurst, J.; Haas, F.; Manfredi, G.; Hervieux, P.-A. High-harmonic generation by nonlinear resonant excitation of surface plasmon modes in metallic nanoparticles. *Phys. Rev. B: Condens. Matter Mater. Phys.* **2014**, *89*, 161111.
(48) Hurst, J.; Lévêque-Simon, K.; Hervieux, P.-A.; Manfredi, G.; Haas, F. High-harmonic generation in a quantum electron gas trapped in a nonparabolic and anisotropic well. *Phys. Rev. B: Condens. Matter Mater. Phys.* **2016**, *93*, 205402.
(49) Ginzburg, P.; Krasavin, A. V.; Wurtz, G. A.; Zayats, A. V. Nonperturbative hydrodynamic model for multiple harmonics generation in metallic nanostructures. *ACS Photonics* **2015**, *2*, 8−13.
(50) Krasavin, A. V.; Ginzburg, P.; Wurtz, G. A.; Zayats, A. V. Nonlocality-driven supercontinuum white light generation in plasmonic nanostructures. *Nat. Commun.* **2016**, *7*, 11497.
(51) Aouani, H.; Navarro-Cia, M.; Rahmani, M.; Sidiropoulos, T. P. H.; Hong, M.; Oulton, R. F.; Maier, S. A. Multiresonant broadband optical antennas as efficient tunable nanosources of second harmonic light. *Nano Lett.* **2012**, *12*, 4997−5002.
(52) Thyagarajan, K.; Rivier, S.; Lovera, A.; Martin, O. J. Enhanced second-harmonic generation from double resonant plasmonic antennae. *Opt. Express* **2012**, *20*, 12860−12865.
(53) Chen, P.-Y.; Argyropoulos, C.; Alù, A. Enhanced nonlinearities using plasmonic nanoantennas. *Nanophotonics* **2012**, *1*, 221−233.
(54) Berthelot, J.; Bachelier, G.; Song, M.; Rai, P.; des Francs, G. C.; Dereux, A.; Bouhelier, A. Silencing and enhancement of second-harmonic generation in optical gap antennas. *Opt. Express* **2012**, *20*, 10498−10508.
(55) Haus, J. W.; de Ceglia, D.; Vincenti, M. A.; Scalora, M. Nonlinear quantum tunneling effects in nanoplasmonic environments: two-photon absorption and harmonic generation. *J. Opt. Soc. Am. B* **2014**, *31*, A13−A19.
(56) Terhune, R. W.; Maker, P. D.; Savage, C. M. Optical harmonic generation in calcite. *Phys. Rev. Lett.* **1962**, *8*, 404.
(57) Lee, C. H.; Chang, R. K.; Bloembergen, N. Nonlinear electroreflectance in silicon and silver. *Phys. Rev. Lett.* **1967**, *18*, 167−170.
(58) Aktsipetrov, O. A.; Fedyanin, A. A.; Mishina, E. D.; Rubtsov, A. N.; van Hasselt, C. W.; Devillers, M. A. C.; Rasing, T. dc-electric-field-induced second-harmonic generation in Si (111)-SiO 2-Cr metal-oxide-semiconductor structures. *Phys. Rev. B: Condens. Matter Mater. Phys.* **1996**, *54*, 1825.
(59) Castro-Lopez, M.; Brinks, D.; Sapienza, R.; van Hulst, N. F. Aluminum for nonlinear plasmonics: resonance-driven polarized luminescence of Al, Ag, and Au nanoantennas. *Nano Lett.* **2011**, *11*, 4674−4678.
(60) Narang, P.; Sundararaman, R.; Jermyn, A. S.; Goddard, W. A.; Atwater, H. A. Cubic Nonlinearity Driven Up-Conversion in High-Field Plasmonic Hot Carrier Systems. *J. Phys. Chem. C* **2016**, *120*, 21056−21062.
(61) Knight, M. W.; King, N. S.; Liu, L.; Everitt, H. O.; Nordlander, P.; Halas, N. J. Aluminum for plasmonics. *ACS Nano* **2014**, *8*, 834−840.
(62) Maidecchi, G.; Gonella, G.; Proietti Zaccaria, R.; Moroni, R.; Anghinolfi, L.; Giglia, A.; Nannarone, S.; Mattera, L.; Dai, H.-L.; Canepa, M. Deep ultraviolet plasmon resonance in aluminum nanoparticle arrays. *ACS Nano* **2013**, *7*, 5834−5841.
(63) Hobbs, R. G.; Manfrinato, V. R.; Yang, Y.; Goodman, S. A.; Zhang, L.; Stach, E. A.; Berggren, K. K. High-energy surface and volume plasmons in nanopatterned sub-10-nm aluminum nanostructures. *Nano Lett.* **2016**, *16*, 4149.
(64) Boyd, R. W. *Nonlinear Optics*; Academic Press, 2003.
(65) Calvayrac, F.; Reinhard, P.-G.; Suraud, E.; Ullrich, C. Nonlinear electron dynamics in metal clusters. *Phys. Rep.* **2000**, *337*, 493−578.
(66) Marques, M. A. L.; Gross, E. K. U. Time-dependent density functional theory. *Annu. Rev. Phys. Chem.* **2004**, *55*, 427−455.
(67) de Heer, W. A.; Milani, P.; Chatelain, A. Nonjellium-to-jellium transition in aluminum cluster polarizabilities. *Phys. Rev. Lett.* **1989**, *63*, 2834−2836.
(68) Lang, N. D.; Kohn, W. Theory of metal surfaces: Work function. *Phys. Rev. B* **1971**, *3*, 1215−1223.
(69) Marinica, D.; Kazansky, A.; Nordlander, P.; Aizpurua, J.; Borisov, A. G. Quantum plasmonics: Nonlinear effects in the field enhancement of a plasmonic nanoparticle dimer. *Nano Lett.* **2012**, *12*, 1333−1339.
(70) Zuloaga, J.; Prodan, E.; Nordlander, P. Quantum description of the plasmon resonances of a nanoparticle dimer. *Nano Lett.* **2009**, *9*, 887−891.
(71) Varas, A.; García-González, P.; Feist, J.; García-Vidal, F. J.; Rubio, A. Quantum plasmonics: from jellium models to ab initio calculations. *Nanophotonics* **2016**, *5*, 409−426.
(72) Prangsma, J. C.; Kern, J.; Knapp, A. G.; Grossmann, S.; Emmerling, M.; Kamp, M.; Hecht, B. Electrically connected resonant optical antennas. *Nano Lett.* **2012**, *12*, 3915−3919.
(73) Kern, J.; Kullock, R.; Prangsma, J.; Emmerling, M.; Kamp, M.; Hecht, B. Electrically driven optical antennas. *Nat. Photonics* **2015**, *9*, 582−586.
(74) Cox, J. D.; de Abajo, F. J. G. Electrically tunable nonlinear plasmonics in graphene nanoislands. *Nat. Commun.* **2014**, *5*, 5725.
(75) Boyd, R. W.; Shi, Z.; Leon, I. D. The third-order nonlinear optical susceptibility of gold. *Opt. Commun.* **2014**, *326*, 74−79.
(76) Lassiter, J. B.; Chen, X.; Liu, X.; Cirací, C.; Hoang, T. B.; Larouche, S.; Oh, S.-H.; Mikkelsen, M. H.; Smith, D. R. Third-Harmonic Generation Enhancement by Film-Coupled Plasmonic Stripe Resonators. *ACS Photonics* **2014**, *1*, 1212−1217.
(77) Nezami, M. S.; Yoo, D.; Hajisalem, G.; Oh, S.-H.; Gordon, R. Gap Plasmon Enhanced Metasurface Third-Harmonic Generation in Transmission Geometry. *ACS Photonics* **2016**, *3*, 1461−1467.
(78) Liu, T.-M.; Tai, S.-P.; Yu, C.-H.; Wen, Y.-C.; Chu, S.-W.; Chen, L.-J.; Prasad, M. R.; Lin, K.-J.; Sun, C.-K. Measuring plasmon-resonance enhanced third-harmonic $\chi^{(3)}$ of Ag nanoparticles. *Appl. Phys. Lett.* **2006**, *89*, 043122.
(79) Uchida, K.; Kaneko, S.; Omi, S.; Hata, C.; Tanji, H.; Asahara, Y.; Ikushima, A. J.; Tokizaki, T.; Nakamura, A. Optical nonlinearities of a high concentration of small metal particles dispersed in glass: copper and silver particles. *J. Opt. Soc. Am. B* **1994**, *11*, 1236−1243.
(80) Zhu, W.; Esteban, R.; Borisov, A. G.; Baumberg, J. J.; Nordlander, P.; Lezec, H. J.; Aizpurua, J.; Crozier, K. B. Quantum mechanical effects in plasmonic structures with subnanometre gaps. *Nat. Commun.* **2016**, *7*, 11495.
(81) Zhang, P.; Feist, J.; Rubio, A.; García-González, P.; García-Vidal, F. J. Ab initio nanoplasmonics: The impact of atomic structure. *Phys. Rev. B: Condens. Matter Mater. Phys.* **2014**, *90*, 161407.

DOI: 10.1021/acsphotonics.6b00953
ACS Photonics 2017, 4, 613−620

(82) Haus, J. W.; de Ceglia, D.; Vincenti, M. A.; Scalora, M. Quantum conductivity for metal-insulator-metal nanostructures. *J. Opt. Soc. Am. B* **2014**, *31*, 259−269.

DOI: 10.1021/acsphotonics.6b00953
ACS Photonics 2017, 4, 613−620